

This manuscript was accepted and published by *Energy & Fuels*, a journal of the American Chemical Society.

Publication data of the final, corrected work:

Várhegyi, G.; Szabó, P.; Jakab, E.; Till, F.; Richard J-R.: Mathematical modeling of char reactivity in Ar-O<sub>2</sub> and CO<sub>2</sub>-O<sub>2</sub> mixtures. *Energy Fuels* **1996**, *10*, 1208-1214. doi: [10.1021/ef950252z](https://doi.org/10.1021/ef950252z)

---

## Mathematical Modeling of Char Reactivity in Ar-O<sub>2</sub> and CO<sub>2</sub>-O<sub>2</sub> Mixtures

Gábor Várhegyi,\* Piroska Szabó, Emma Jakab, Ferenc Till

Hungarian Academy of Sciences,

Research Laboratory for Inorganic Chemistry,

P.O.Box 132, Budapest 1518, Hungary

\*Email: [varhegyi.gabor@t-online.hu](mailto:varhegyi.gabor@t-online.hu) or [gvarhegyi@gmail.com](mailto:gvarhegyi@gmail.com)

and

Jean–Robert Richard

C.N.R.S., Laboratoire de Combustion et Systèmes Réactifs

1C Avenue de la Recherche Scientifique

45071 Orléans Cedex 2

### ABSTRACT

The kinetics of the coal char + O<sub>2</sub> reaction was studied by thermogravimetry. Low sample masses were employed to ensure an approximate kinetic regime. Special emphasis was placed on clarifying how the recirculation of the flue gases (i.e. the presence of a high amount of CO<sub>2</sub> at low O<sub>2</sub> concentrations) affects the reactivity. The ambient gas concentrations varied from 100% O<sub>2</sub> to 5% O<sub>2</sub> in CO<sub>2</sub> or Ar. A semi-empirical model is presented which can approximate the reactivity changes during the conversion and takes into account the heterogeneity of the samples. A least squares evaluation procedure resulted in a good fit to the experimental data over a wide variety of temperature programs and ambient gas concentrations. The overall burn-off time of the samples varied from eight minutes to three hours depending on the experimental conditions. The reaction rate was found to be proportional to the O<sub>2</sub> concentration of the ambient gas and was not influenced by the presence of high amounts of CO<sub>2</sub>. The reaction started with a sharp acceleration period indicating an initial activation of the char surface.

## Introduction

The authors participated in the Pressurized Pulverized Coal Combustion Project Area of the JOULE II program. The research aimed at an assessment of the viability and technical merits of pulverized coal combustion in an atmosphere of recycled flue gas and oxygen. Seven research groups collaborated to clarify the details of pollutant formation under various experimental conditions. One particular task was a study of the fundamental properties of selected coal and char samples by an atmospheric pressure thermobalance – mass spectrometer system. This technique provided information about char reactivity and pollutant formation under experimental conditions at which the sample temperature is well defined and the influence of the mass transfer can be reduced to a negligible level. Although the primary goal of the atmospheric pressure studies was to aid the interpretation of the high pressure experiments of the project participants, we think that our results are interesting to other researchers of the field, as well. The present paper deals with the reaction kinetic evaluation of our thermogravimetric curves. Particular efforts were made to clarify how the recirculation of the flue gases (i.e. the presence of a high amount of CO<sub>2</sub> at low O<sub>2</sub> concentrations) affects the kinetics of the char + O<sub>2</sub> reaction.

The combustion of pure model carbons in the kinetic regime can be described by relatively simple theoretical models since the reaction rate is proportional to the surface area of the samples. On this basis elegant mathematical models have been published giving theoretical deductions for the change of the reaction surface as the burn-off proceeds.<sup>1-4</sup> However, subsequent char gasification studies revealed more and more difficulties. Hurt et al.<sup>5</sup> proved the special role of microporous surface area in carbon gasification processes. Lizio et al.<sup>6-7</sup> made a clear distinction between reactive surface area (RSA), active surface area (ASA) and total surface area (TSA). Kyotani et al.<sup>8</sup> presented an interesting molecular structure model on carbon reactivity. Miura et al.<sup>9-10</sup> reported two-step reactions in temperature programmed air gasification of coal chars. Silveston<sup>11</sup> explained this phenomena by assuming a “reactive carbon” component which forms during the preparation of the chars.

The studies listed above clearly indicate that the coal char + O<sub>2</sub> reaction is very complex. An investigation of the subtle, molecular level-details of the oxidation chemistry was beyond the scope of this work. On the other hand, we wished to avoid such oversimplifications as the description of the whole process by a “pseudo first order” reaction.<sup>12</sup> The aim of our research was to find a versatile semi-empirical model which can approximate reactivity changes during conversion and which takes into account the char heterogeneity reported by Miura et al.<sup>9-10</sup> and Silveston.<sup>11</sup>

## Experimental Section

**Samples.** Two typical European high-volatile bituminous coals, a Polish (*Arkadia*) and a German (*Westerholt*) coal were selected for the investigations. A French lignite of great future economic potential

from the *Gardanne* region was also included in the study. (See Table 1.) The chars were prepared by heating to 950°C in inert atmosphere at a rate of 10°C/min and holding at 950°C for 30 min. The samples were ground in an agate mortar and a fraction between 120 and 200 µm was used. The ultimate analysis was carried out by the *Central Research Institute for Chemistry of the Hungarian Academy of Sciences* using a Fisons EA1108 Elemental Analyzer. Since the primary aim of the study was feedstock characterization for large scale, industry-oriented experiments, the room-temperature manipulation and storage of the chars were not made under inert gas. As a consequence, the inorganic oxides formed during char preparation could react with the CO<sub>2</sub> and H<sub>2</sub>O content of the air. A high amount (9% db) of carbonate CO<sub>2</sub> was found in the Gardanne lignite char by thermogravimetric - mass spectrometric analysis<sup>13</sup> in argon flow. The temperature and shape of the corresponding DTG (-dm/dt) peak were characteristic to calcium carbonate powders. The lignite contained approximately 12% carbonate CO<sub>2</sub>.

**Table 1. Characterization data for the chars and their parent coals<sup>a</sup>**

	C	H	N	S	O <sup>b</sup>	Ash	Volatile matter
Gardanne lignite	48.9	3.3	1.3	2.5	17.9	26.1	42.5
Arkadia coal	74.8	4.8	1.5	0.6	8.8	9.5	30.4
Westerholt coal	69.0	4.4	1.5	1.2	8.4	15.5	33.9
Gardanne char	57.7	0.5	1.4	2.2	5.5	32.7	–
Arkadia coke	84.9	0.3	1.6	0.4	1.5	11.3	–
Westerholt coke	63.1	0.2	1.6	0.7	2.3	32.1	–

<sup>a</sup> Dry basis (%)

<sup>b</sup> By difference. (See comments in the text.)

**Equipment, Ambient Gases and Temperature Programs.** A Perkin Elmer TGS-2 thermobalance was used. Its high resolution (0.1 µg), a stable gas flow control and a high precision digital to analogue converter allowed the use of small sample sizes (0.5 – 4 mg) which were needed to approach closely the kinetic regime of combustion.

To check the effects of CO<sub>2</sub> on the char oxidation kinetics, CO<sub>2</sub> – O<sub>2</sub> experiments were compared with Ar – O<sub>2</sub> experiments. Here argon served as an inert diluent. Note that the heat conductivity and gas diffusion is almost identical in Ar and CO<sub>2</sub>. The effects of the following ambient gas compositions have been investigated:

5% O<sub>2</sub> + 95% Ar, 10% O<sub>2</sub> + 90% Ar, 15% O<sub>2</sub> + 85% Ar, 29% O<sub>2</sub> + 71% Ar,  
 5% O<sub>2</sub> + 95% CO<sub>2</sub>, 10% O<sub>2</sub> + 90% CO<sub>2</sub>, 15% O<sub>2</sub> + 85% CO<sub>2</sub>, 29% O<sub>2</sub> + 71% CO<sub>2</sub>,  
 100% O<sub>2</sub>, and 100% CO<sub>2</sub>.

Test experiments were carried out in He – O<sub>2</sub> mixtures, too. High purity gases were mixed by ASM “AFC-260” flow controllers. One particular composition, 29% O<sub>2</sub> + 71% Ar was purchased from Messer Griesheim Hungary Co. The usual gas flow rate in the TGA furnace was 140 ml/min.

The following temperature programs were employed:

- Linear heating at rates of 10, 20 and 50°C/min
- Long isothermal sections reached by a heating of 25°C/min. The isothermal experiments were terminated by a 10°C/min ramp to 900°C
- Cyclic temperature programs, where each cycle consisted of two isothermal steps connected by 20°C/min linear heating sections and a quick cool-down near to room temperature. The last cycle ended with heating to 900°C.

Four typical temperature programs are shown in Figure 1. The aim of the isothermal and cyclic experiments was to check whether the same reaction kinetic behavior occurs at low and high reaction rates. Consequently, the temperatures of the isothermal sections were selected such that the reaction should require times in the order of 1 – 3 hours. These experiments were carried out in 71% Ar – 29% O<sub>2</sub>. The following temperature values have been selected for the isothermal sections: 455, 470 and 480°C (Gardanne chars); 500, 505 and 513°C (Westerholt coke); 495, 510, 515 and 525°C (Arkadia coke). In an additional Arkadia coke experiment a 2 hour section of 473°C was employed in 100% O<sub>2</sub>.

The 50°C/min experiments provided a “contrast” to the isothermal experiments since higher heating rates increase the reaction rates and shift the reactions to higher temperatures. In this case Ar – O<sub>2</sub> and CO<sub>2</sub> – O<sub>2</sub> ambient gases were used with 5, 10 and 29% O<sub>2</sub> content. At 50°C/min the overall reaction time decreased to approximately 8 minutes.

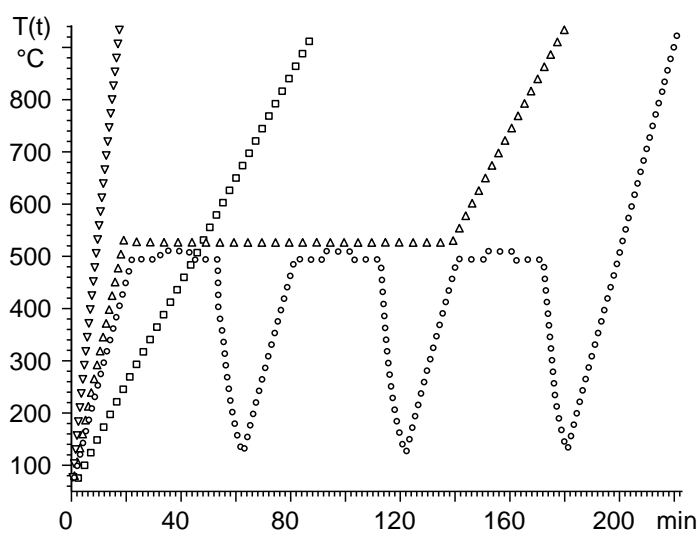


**Figure 1:** Temperature programs used in the Arkadia coke experiments. From left to right: 50°C/min heating ( $\nabla$ ); 10°C/min heating ( $\square$ ); temperature program with an isothermal section of 2 hours at 525°C ( $\Delta$ ); and cyclic heating ( $\circ$ ).

**Sample Mass.** Small samples (0.5 – 4 mg) were evenly distributed in a sample pan with a diameter of 6 mm. Test experiments with different sample sizes were carried out and the normalized reaction rate curves ( $-dm/dt$  as a function of time) were compared. When the sample mass was too high, the curves showed sharper peaks due to considerable self heating. At 10°C/min, in an atmosphere of 29 % oxygen, sample masses of 2 –

4 mg proved to be sufficiently small to avoid significant self heating. When the ambient gas was 100% oxygen, 0.6 – 1 mg sample masses were employed. The high heating rate experiments also required lower sample masses, 0.4 – 0.8 mg, because the reaction rate is roughly proportional to the heating rate. (Cf. Figures 2/a and 2/b.) Arkadia coke appeared to be more inclined to self-heating than the other two chars.

**Calculations.** FORTRAN and C++ programs running under DOS and Windows, respectively, have been developed. The corresponding numerical methods were described earlier.<sup>14–16</sup>

## The Mathematical Model

As discussed in the *Introduction*, several complicating factors arise in the coal char + O<sub>2</sub> reaction, of which the following two appear to be the most important:

- (i) Coal chars may be composed of parts with different properties.
- (ii) The reactivity of a unit surface area may vary as the sample is burning out.

A semi-empirical model has been developed for the approximate description of these phenomena. To include the char heterogeneity into the model, we assumed that a coal char sample can be a mixture of components with different reactivity:

$$m(t) \cong \sum_{j=1}^n c_j [1 - \alpha_j(t)] + \text{const} \quad (m(0) = 1) \quad (1)$$

where  $t$  is time,  $m$  is the sample mass normalized by the initial sample mass,  $n$  is the number of components,  $c_j$  is the fraction of combustibles in component  $j$ , and  $\alpha_j(t)$  is the reacted fraction (fractional burn-off) of component  $j$  in time  $t$ . The term denoted by *const* is the normalized amount of the solid residues (minerals) at the end of the experiment.

A separate equation is used for each component to describe the dependence of the reaction rate on the temperature and on the fractional burn-off:

$$d\alpha_j/dt = A_j \exp(-E_j/RT) g(P_{O_2}, P_{CO_2}) f_j(\alpha_j) \quad (2)$$

where  $A_j$  and  $E_j$  are preexponential factor and activation energy type quantities, while  $g$  and  $f$  represent empirical functions.  $g$  expresses the effects of the ambient gas composition and  $f$  describes the change of the surface area and the surface reactivity as a function of the fractional burn-off.

The evaluation of the experiments revealed that  $g(P_{O_2}, P_{CO_2})$  is proportional to  $P_{O_2}$  and does not depend on  $P_{CO_2}$ . Merging the proportionality constant into the preexponential factors in the usual way, we obtain:

$$g(P_{O_2}, P_{CO_2}) = P_{O_2} \quad (3)$$

For the deduction of a suitable form for the  $f_j(\alpha_j)$  functions we considered the kinetic equation recommended by Chornet et al<sup>17</sup>:

$$d\alpha/dt = k \alpha^a (1-\alpha)^b \quad (4)$$

where  $a$  and  $b$  are non-negative empirical parameters having no direct physical meaning. Equation (4) has been successfully applied for the kinetic modeling of coal gasification, as well.<sup>18</sup> It has a serious drawback, however: the solution of a differential equation of this type is  $\alpha(t) \equiv 0$  if  $\alpha(0) = 0$ . From a physical point of view, we should look for  $f_j(\alpha_j)$  functions which provide some finite value for the reactivity at the beginning of the reaction, too. Hence we introduced a third parameter,  $z$ , into equation (4) and obtained the following empirical functions for equation (2):

$$f_j(\alpha_j) \cong (\alpha_j + z_j)^{a_j} (1 - \alpha_j)^{b_j} / F_j \quad (5)$$

Here  $F_j$  normalizes  $f_j(\alpha_j)$ . We defined  $F_j$  such that the maximum of  $f_j(\alpha_j)$  equals 1. Note that  $f_j(\alpha_j)$  reaches its maximum at

$$\begin{aligned} \alpha_j &= (a_j - b_j z_j) / (a_j + b_j) & (a_j - b_j z_j \geq 0) \\ \alpha_j &= 0 & (a_j - b_j z_j < 0) \end{aligned} \quad (6)$$

Hence the actual values of  $F_j$  can easily be calculated. Since  $z_j$  served to keep  $f_j(0)$  at a non-zero value,  $z_j$  was forced to remain higher than zero during the evaluation. (An arbitrarily chosen lowest limit,  $10^{-5}$  was used for this purpose.)

Note that equation (5) can approximate a wide variety of functions from monotonously descending curves to functions having a maximum at any selected  $\alpha_j$  in interval (0, 1). Due to the versatility of the formula selected, the  $f_j(\alpha_j)$  functions can formally approximate the physical and chemical heterogeneity of a reaction surface as far as the temperature dependence of the char + O<sub>2</sub> reaction is approximately the same on the different parts of the surface. Coal chars may be composed of an endless number of physically or chemically different particles. Nevertheless, the evaluation of the experiments revealed that the Gardanne lignite char could be adequately described by assuming a single component in equation (1) while the Arkadia and Westerholt cokes required the assumptions of two components. This behavior may be due to the averaging capabilities of the  $f_j(\alpha_j)$  functions employed.

It may be interesting to note that the two-component behavior of the Arkadia and Westerholt cokes is well reflected by the shape of their experimental  $-dm/dt$  functions. (See Figures 2/a – 2/b.) The Gardanne lignite char also evidenced a small second peak, but it was attributed to the thermal decomposition of a mineral calcium carbonate component. When the same experiments were repeated in ambient gases containing high amounts of CO<sub>2</sub>, this small peak shifted to a much higher temperature. (See the curve represented by symbols O in Figure 2/b.) It is well known that the thermal decomposition of CaCO<sub>3</sub> is

extremely sensitive to the presence of CO<sub>2</sub> in the ambient gas<sup>19</sup> hence its mathematical modeling should include sophisticated equations for mass transport and backward reactions. The investigation of this problem was beyond the scope of the present study. We restricted the kinetic evaluation of the Gardanne char experiments to temperature domains below the carbonate decomposition.

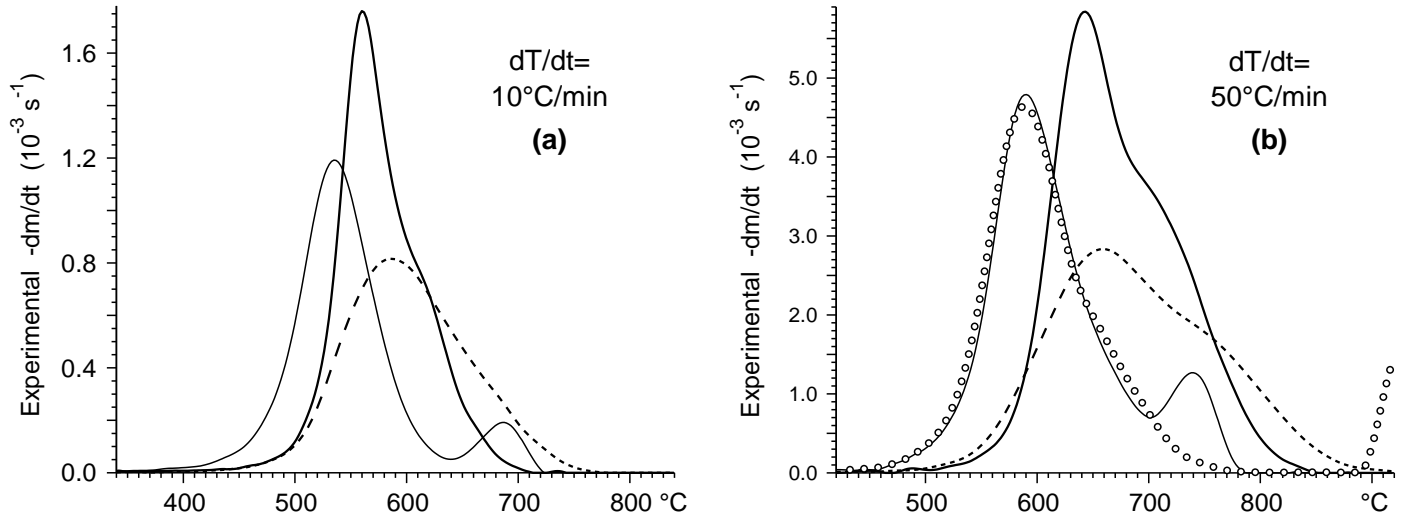


**Figure 2:** Comparison of the normalized mass loss rate of the samples in a flow of 29% O<sub>2</sub> + 71% Ar at 10°C/min (a) and 50°C/min (b), respectively. Notation: Gardanne lignite char (—), Arkadia coke (—) and Westerholt coke (- - -). Figure 1/b shows the behavior of the Gardanne char in 29% O<sub>2</sub> + 71% CO<sub>2</sub> too (o).

### Determination of the Unknown Parameters

The method of least squares was employed. Denoting the  $i$ th point on the  $k$ th experimental curve by  $m^{\text{obs}}(i,k)$ , we search for those parameters which minimize

$$S = \sum_{k=1}^M \sum_{i=1}^{N_j} [m^{\text{calc}}(i,k) - m^{\text{obs}}(i,k)]^2 / N_j / M \quad (7)$$

Here  $M$  (1 or 5) is the number of experimental curves used in the given run of evaluation while  $N_j$  ( $\approx 200$ ) is the number of points on the  $j$ th experimental curve. Equations (1–2) were solved numerically along the measured  $T(t)$  function in each iteration step of the minimization.<sup>15</sup>

In earlier work<sup>15,16</sup> we showed that different thermoanalytical experiments cannot be described by *exactly* the same parameters due to such measurement errors which distort the shape and temperature of the experimental curves. It means that a slight variance of the model parameters should be allowed to formally describe this type of errors. In the present case the preexponential factors and the  $c_j$  coefficients were allowed to have some scattering. The scattering resulted from the following sources: (i) coal char particles always show some heterogeneity; (ii) due to this heterogeneity, the mineral matter in the small samples of this study varied by 1 – 2 % from experiment to experiment; (iii) the kinetic evaluation of the Gardanne lignite char curves was disturbed by the presence of a prominent carbonate decomposition peak; (iv) the measurement of

the sample temperature always has some uncertainty in thermal analysis; (v) the mixing of the gases also involves small experimental errors.

Errors (i) - (iii) distort the  $c_j$  coefficients and affect the kinetic parameters. The gas composition errors can formally be compensated by small  $\delta \log A_j$  changes in models based on equation (2). The variation of  $\log A_j$  can formally describe temperature errors, too, as outlined in the *Discussion of the Results*. The techniques used to obtain scattering values for  $\log A_j$  and  $c_j$  will be briefly summarized in a separate paragraph after the overview of the whole evaluation process.

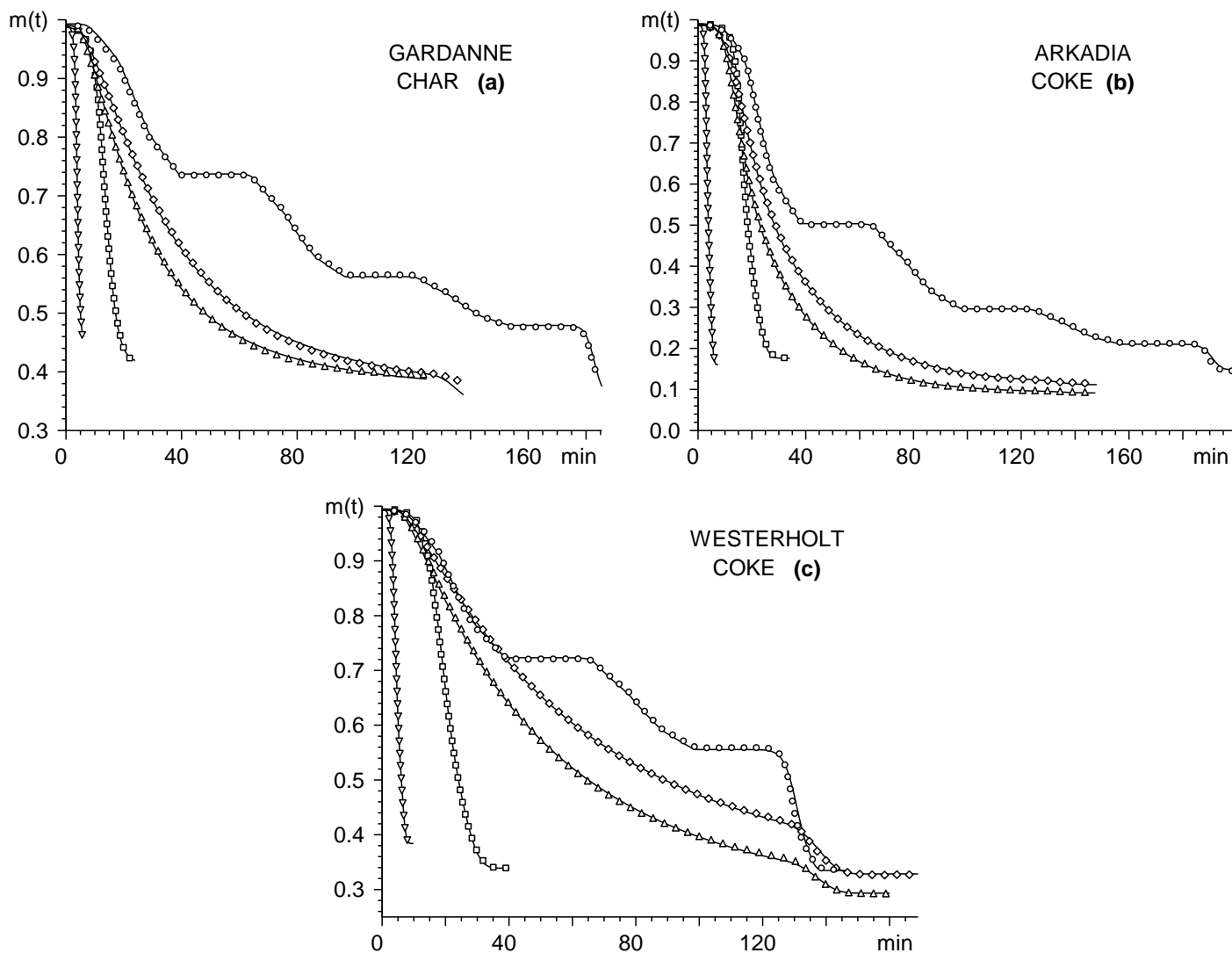


**Figure 3:** Simultaneous evaluation of five experiments in 71% Ar + 29% O<sub>2</sub> with Gardanne lignite char (a), Arkadia coke (b) and Westerholt coke (c). The experimental curves, represented by symbols, differ from each other by the heating programs employed: 50°C/min heating ( $\nabla$ ); 10°C/min heating ( $\square$ ); two temperature programs with 2-hour isothermal sections ( $\diamond$  and  $\triangle$ ); and cyclic heating (o). (See Figure 1.) The solid lines show the best fitting simulated curves. Only the domains included into the least squares sum were plotted and a common  $t=0$  was set on the time axis.

For each sample 25 - 39 experiments were available. The simultaneous least squares evaluation of so many data would have required an enormous computational effort. On the other hand, a single experiment



did not contain enough information to determine all the unknown parameters of the model. As a compromise, the calculations have been carried out in two steps:

Step I: Five experiments with very different temperature programs were evaluated simultaneously for each char. This procedure yielded unique values for  $E_j$  and the parameters of functions  $f_j(\alpha_j)$ . (As mentioned above,  $\log A_j$  and  $c_j$  were allowed to scatter slightly.) The temperature programs and the fit between the calculated and the experimental curves are shown in Figures 3/a – 3/c.

Step II: Using the activation energies and the parameters of the  $f_j(\alpha_j)$  functions obtained in Step I as fixed values, all of the 92 TG curves were evaluated one by one. The means and deviations of the parameters obtained by this procedure are listed in Table 2.

Figures 4/a – 4/c illustrate the performance of the model at ambient gases containing 0, 29 and 90% CO<sub>2</sub>, respectively. Here the solution of the model equations were plotted at three different parameter sets: mean parameters obtained in Step I (····); mean parameters calculated from all experiments (---); and best fitting parameters for the given experiment (—).

**Table 2. Results of the kinetic evaluation<sup>a</sup>**

Sample	Number of experiments	Fit <sup>b</sup> %	E kJ/mol	$\log_{10} A$ (s Mpa) <sup>-1</sup>	c	a	b	z	F
Gardanne char	25	0.8±0.6	147	8.43±0.06	0.59±0.03	1.52	0.42	0.0147	0.37
Arkadia	28	0.4±0.3	136	7.55±0.07	0.40±0.01	1.58	0.76	0.0011	0.23
coke <sup>c</sup>			111	5.42±0.06	0.45±0.02	0.99	0.35	0.0039	0.47
Westerholt	39	0.5±0.4	135	7.17±0.05	0.45±0.02	1.23	0.25	10 <sup>-5</sup>	0.51
coke <sup>c</sup>			104	4.64±0.05	0.23±0.01	0.98	0.43	10 <sup>-5</sup>	0.42

<sup>a</sup> The '±' signs separate the means and standard deviations of scattering values.

<sup>b</sup> The deviation between the observed and the simulated thermogravimetric curves is expressed as percent of the initial sample mass.

<sup>c</sup> A separate parameter set is given for each component. [See equation (1).]

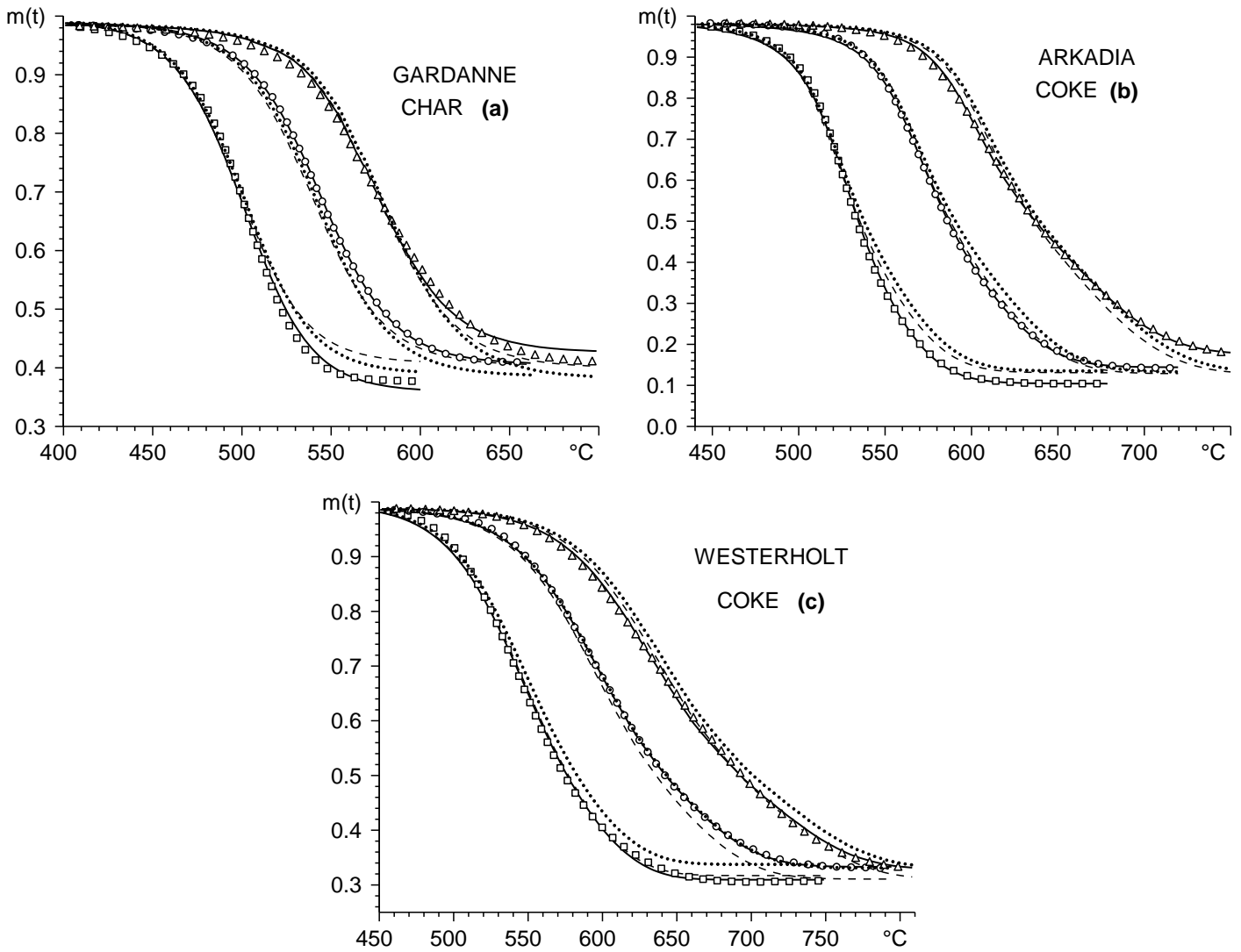


**Figure 4:** Modeling experiments at ambient gas compositions 100% O<sub>2</sub> ( $\square$ ), 29% O<sub>2</sub> + 71% CO<sub>2</sub> ( $\circ$ ) and 10% O<sub>2</sub> + 90% CO<sub>2</sub> ( $\Delta$ ). Heating rate: 10 $^{\circ}\text{C}/\text{min}$ . For each experiment, the solution of the model equations is plotted at three different parameter sets: mean parameters obtained from the experiments of Figures 3a – 3c ( $\cdots$ ); mean parameters calculated from all experiments of the study ( $---$ ); and best fitting parameters for the given experiment ( $—$ ).

**Techniques for the Determination of Scattering Parameter Values.** Each experimental curve has different values for  $\log A_j$  and  $c_j$  and common values for  $E_j$  and the parameters of functions  $f_j(\alpha_j)$ . Since the behavior of the Gardanne lignite char could be approximated by one component in equation (1), the simultaneous evaluation of five experiments in Step I required a least squares minimization by 14 unknown parameters. (One  $\log A$  and  $c$  for each curve and common values for  $E$ ,  $a$ ,  $b$  and  $z$ .) In Step II all experiments were evaluated separately and only two unknown values,  $\log A$  and  $c$ , were determined for each experiment.

The Arkadia and Westerholt cokes were regarded as mixtures of two components. Consequently, Step I of the evaluation required minimizations by 28 unknown parameters. It turned out that very good fits can be obtained at chemically meaningless  $E_j$  and an enormous scattering of  $\log A_j$  and  $c_j$ . The convergence to such minima was eliminated by excluding solutions with strongly different values for a given parameter. For this purpose a “penalty” was added to the objective function of the minimization:

$$penalty = \sum_{k=1}^5 \sum_{j=1}^2 w_{\log A} (\delta \log A_{j,k})^2 + w_c (\delta c_{j,k})^2 \quad (8)$$

where subscripts  $k$  and  $j$  indicate the  $k$ th experiment and the  $j$ th component while  $\delta \log A_{j,k}$  and  $\delta c_{j,k}$  are the deviations of  $\log A_{j,k}$  and  $c_{j,k}$  from the corresponding average parameter values,  $\langle \log A_j \rangle$  and  $\langle c_j \rangle$ , respectively. Averages  $\langle \log A_j \rangle$  and  $\langle c_j \rangle$  were recalculated at each function evaluation during the numerical minimization of the  $S + penalty$  function, where  $S$  is the least squares sum defined by (7). Weight factors  $w_{\log A}$  and  $w_c$  served to control the scattering of the parameters. Test calculations carried out in the present work as well as in earlier kinetic studies<sup>14–15</sup> showed that the results of the minimization are not sensitive to the exact choice of the weight factors in the penalty terms. Values  $w_{\log A}=0.01$  and  $w_c=0.1$  resulted in reasonable fit and scattering.

In Step II of the evaluation no constraints were employed for the scattering of  $\log A_1$  and  $\log A_2$ . On the other hand, the determination of the values of  $c_1$  and  $c_2$  required a certain caution. From a mathematical point of view, the splitting of an  $m(t)$  function into two components by equation (1) is equivalent to the resolution of the derivative function,  $-dm/dt$  into two partial peaks. However, the partial peaks of the curves drawn by dashed and bold solid lines in Figure 2/a highly overlapped each other. Their reliable numerical resolution required the use of information from the less overlapping curves of Figure 2/b and from isothermal experiments, as done in Step I. Hence the values of  $c_1$  and  $c_2$  in Step II were forced to remain close to the  $\langle c_1 \rangle$  and  $\langle c_2 \rangle$  averages obtained in Step I of the evaluation. (See Table 2 for the results of these calculations.)

To check the reliability of the process, all evaluations of Step II were repeated without the use of any constraints. This procedure yielded averages and deviations of  $\log A_1$  and  $\log A_2$  very close to the corresponding values of Table 2 while coefficients  $c_1$  and  $c_2$  revealed a higher scattering, in the order of 0.05.

The necessity of a constraint of type (8) indicates that we could not find a *best* set of parameters. Nevertheless, the parameters obtained in the evaluation provided good fits for experiments in a wide range of experimental conditions, as will be discussed in the next paragraph.

## Discussion of the Results

**Negligible Effect of CO<sub>2</sub> on Reaction Rates.** We have not observed any special effect when we replaced argon by CO<sub>2</sub>. This may be due to the fact that the char + CO<sub>2</sub> reactions have lower rates than the char oxidation. As a check, we measured the behavior of the Westerholt coke in CO<sub>2</sub> at a heating of 10°C/min. The reaction started around 800°C and reached a reaction rate of  $2 \times 10^{-5} \text{ s}^{-1}$  around 900°C. At oxygen levels of 5 and 29% the same reaction rate was reached around 450 and 500°C, respectively.

**Shape of the  $f(\alpha)$  functions.** Since the integration of the differential equations along the  $T(t)$  temperature programs was carried out from temperatures below the start of mass loss, the very beginning of

the burn-off was also included in the evaluation. In studies based only on isothermal kinetics,<sup>5,20-23</sup> one cannot deal with the events taking place before reaching and stabilizing the experimental conditions of the isothermal reaction. When the reactive gas is introduced to a preheated sample, a certain time is needed to reach a homogeneous oxygen distribution in the reactor. If the sample is moved into a hot, oxygen-containing ambient or if a fast heating is applied, then the temperature stabilization in the sample causes problems. These can be overcome by the controlled heating of the sample in the presence of the reactive gas and by the appropriate kinetic evaluation of the corresponding data, as described in the paper.

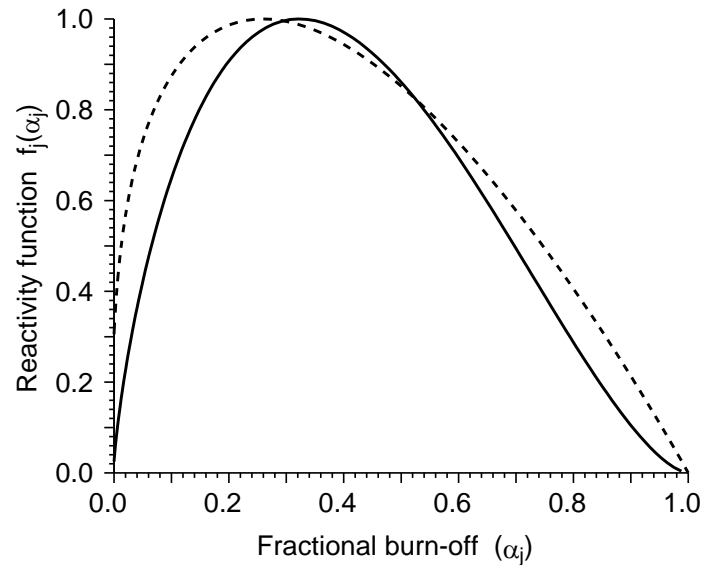


**Figure 5:** Functions  $f_1(\alpha_1)$  (—) and  $f_2(\alpha_2)$  (---) for Arkadia coke. These functions formally approximate the changes in the area and reactivity of the reaction surface as the char burns off. (See equations (1), (2) and (5).)

Figure 5 shows that the  $f_j(\alpha_j)$  functions used in the model start with a sharp increase. The maximum-curve character of these functions is much more pronounced than that of the theoretical surface models deduced from pore distribution hypotheses.<sup>1-4</sup> As an explanation, we assume that the burn-off of the samples started with an activation of the char surface. The prolonged heating at 950°C during the preparation of the samples probably stabilized the surfaces. When the reaction starts, the stabilized surface burns down and fresh surfaces with chemical and physical irregularities are formed causing a sharp acceleration at the onset of the combustion. As an alternative explanation, the pronounced initial increase of the  $f_j(\alpha_j)$  functions could have been attributed to the widening of micropores during the gasification. However, Álvarez et al.<sup>23</sup> pointed out in a recent work that a diffusional resistance at the initial stages of gasification should result in a lower, non-constant activation energy.

**Table 3 Selected characteristic temperatures (°C) of the series of experiments used in the reaction kinetic evaluation<sup>a</sup>.**

Sample	Observed T <sub>peak</sub> in 100% O <sub>2</sub> at 10°C/min	Observed T <sub>peak</sub> in 29% O <sub>2</sub> at 50°C/min	Observed T <sub>peak</sub> in 5% O <sub>2</sub> at 10°C/min	Combined domain of the kinetic evaluation
Gardanne char	503	595	610	350 – 740
Arkadia coke	529	643	648	400 – 840
Westerholt coke	543	683	700	400 – 950

<sup>a</sup> T<sub>peak</sub> is the temperature belonging to the highest experimental  $-dm/dt$  value.

**Domains of Validity.** The combined temperature domains of the kinetic evaluation were extremely wide, as shown in the last column of Table 3. These intervals express the distance between the start of the reaction in pure O<sub>2</sub> and the end of the reaction in 5% O<sub>2</sub> at 10°C/min or in 29% O<sub>2</sub> at 50°C/min. Table 3 also includes temperature characteristics of the lower and higher temperature experiments at constant heating rates.

The fits were considerably worse at the lowest oxygen level of the study (5% O<sub>2</sub> in Ar or CO<sub>2</sub>) than in the other cases. Nevertheless, the parameters obtained from the 5% O<sub>2</sub> experiments did not differ significantly from the values belonging to 10 – 100% O<sub>2</sub>, hence the 5% O<sub>2</sub> experiments were also included in the averages and deviations shown in Table 2.

Consequently, a relatively simple model describes the kinetics of the mass loss over a wide range of temperatures and ambient gas concentrations. On the other hand, the chemistry and physics of the coal char + O<sub>2</sub> reaction is known to be very complex. To explain the simplicity of the kinetics observed one can assume that a chemical reaction in the chain of events is much slower than the other partial processes and, in this way, determines the overall reaction rate.

**Scatter of Preexponential Factors.** The standard deviations of log A were around 0.05 – 0.07. As discussed above, this scattering results from several different sources. As a rough approximation, however, we can estimate how much temperature errors would correspond to a given  $\delta \log A$  error if the errors of log A were due only to temperature errors. Let us suppose that some experimental errors result in a combined temperature shift of  $\delta T$  without changing significantly the magnitude of the reaction rates. (Such shifts frequently occur in thermal analysis.) If we evaluate the shifted curve, the apparent value of A is changing by  $\delta A$ . The equation of the shift is

$$(A+\delta A) \exp[-E/R(T+\delta T)] \approx A \exp(-E/RT) \quad (9)$$

hence

$$\delta \ln A \approx -E/RT^2 \delta T \quad (10)$$

In this way the scattering of log A in the Gardanne coke experiments is approximately equivalent with a temperature uncertainty of 6°C. In the case of the Westerholt experiments we got 5°C at the beginning of the process and 10°C at the end. The corresponding values of the Arkadia experiments are higher, 7 and 11°C, respectively.

**Influence of Heat and Mass Transfer.** The effect of the heat and mass transfer was checked by four methods:

- a) Test experiments were carried out at different sample masses (See the Experimental section).
- b) Experiments with burn-off times of about 3 hours were described by approximately the same kinetic parameters as the ones with burn-off times of about 8 min.
- c) Four experiments were carried out in He – O<sub>2</sub> mixtures at 15% and 29% O<sub>2</sub> levels at a linear heating of 10°C/min . (Note that helium enhances both heat and mass conductivity.)
- d) For each sample test experiments were carried out at 70 and 200 ml/min gas flow rates.

In our opinion, test b) alone excludes the possibility of any significant diffusion control. (Note that chemical reactions have higher temperature dependence than the gas diffusion.)

The replacement of argon by helium increased the apparent reaction temperatures. This may be due to the eight times better heat conductivity of the helium, which reduces the self heating of the samples and may alter the temperature difference between the thermocouple and the sample pan. (Note that these are two different sources of errors. In most thermobalances the thermocouple does not have direct contact with the sample pan to increase balance sensitivity and reduce mechanical inertia.) From a kinetic point of view, the reaction rate curves were slightly widened in the He+O<sub>2</sub> experiments, but the shape itself did not change. The kinetic parameters obtained from these experiments did not differ too much from the other experiments, hence they have been included into the means and deviations of Table 2.

The variation of the gas flow rate between 70 and 200 ml/min did not affect the experiments.

The results of the above described tests and a survey of the kinetic parameters of all the 92 experiments together indicated that our experimental conditions reasonably approximate the kinetic regime of the combustion. No signs for a significant diffusion control appeared and the heat transfer problems manifested in the forms of moderate experimental errors which were easy to handle during the kinetic evaluation.

## Conclusions

The mass loss rates did not depend on the CO<sub>2</sub> content of the ambient gas indicating that CO<sub>2</sub> may influence only the secondary reactions of the CO and CO<sub>2</sub> formed.

The reaction rate proved to be proportional to P<sub>O<sub>2</sub></sub>.

A relatively simple model described the kinetics of the mass loss over a wide range of temperatures and ambient gas concentrations.

The least squares curve fitting techniques employed in this study enabled us to obtain information on char heterogeneity by assuming more than one component in the coal chars.

The results indicated that reaction starts with a sharp acceleration period which may be due to an initial activation of the char surface.

**Acknowledgments.** This research was funded by the PECO program of the European Union (contract number JOU2-CT92-0037/CIPD-CT92-5022) and by the Hungarian National Research Fund (OTKA, grant T 016 173). We thank Dr. Eric Croiset for the preparation of the chars. We are grateful to Dr. Ken Matthews, Project Coordinator and Dr. Bernhard Bonn, Project Area Coordinator, for their interest in this work.

## REFERENCES

- (1) Bhatia, S. K; Perlmutter, D. D.: A random pore model for fluid–solid reactions: I. Isothermal kinetic control. *AIChE J.* **1980**, *26*, 379. Bhatia, S. K and Perlmutter, D. D. : A random pore model for fluid–solid reactions: II. Diffusion and transport effects. *AIChE J.* 1981, *27*, 247.
- (2) Gavalas, G. R.: A random capillary model with application to char gasification at chemically controlled rates. *AIChE J.* **1980**, *26*, 577–585
- (3) Reyes, S; Jensen, K. F.: Percolation concepts in modeling of gas–solid reactions. I. Application to char gasification in the kinetic regime. *Chem. Eng. Sci.* **1986**, *41*, 333–340.
- (4) Tseng, H. P; Edgar, T. F.: The Change of the Physical-Properties of Coal Char During Reaction. *Fuel* **1989**, *68*, 114–119.
- (5) Hurt, R. H.; Sarofim, A. F.; Longwell, J. P.: Role of Microporous Surface Area in Uncatalyzed Carbon Gasification. *Energy Fuels* **1991**, *5*, 290–299.
- (6) Lizzio, A. A; Jiang, H.; Radovic, L. R.: On the Kinetics of Carbon (Char) Gasification: Reconciling Models with Experiments. *Carbon* **1990**, *29*, 809–811.
- (7) Radovic, L. R.; Lizzio, A. A.; Jiang, H.: Reactive Surface Area: An Old but New Concept in Carbon Gasification. In *Fundamental Issues in Control of Carbon Gasification Reactivity*, Lahaye, J; Ehrburger, P. Eds.; Kluwer Academic Publishers: The Netherlands, 1991, pp. 235–255.
- (8) Kyotani, T; Leon y Leon C. A; Radovic, L. R.: Simulation of Carbon Gasification Kinetics Using an Edge Recession Model. *AIChE J.* **1993**, *39*, 1178–1184.
- (9) Miura, K.; Makino, M.; Silveston, P.L.: Two-Step Gasification of Flash Pyrolysis and Hydropyrolysis Chars from Low-Rank Canadian Coals. *Energy Fuels* **1990**, *4*, 24–27.

- (10) Miura, K.; Nakamura, H.; Hashimoto, K.: Analysis of 2-Step Reaction Observed in Air Gasification of Coal Through a Temperature-Programmed Reaction Technique. *Energy Fuels* **1991**, *5*, 47–51.
- (11) Silveston, P. L.: Analysis of 2-Step Reaction Observed in Air Gasification of Coal Through a Temperature-Programmed Reaction Technique – Comment. *Energy Fuel* **1991**, *5*, 933–934.
- (12) Cuesta, A.; Martínez–Alonso, A.; Tascón, M. D.: Correlation between Arrhenius Kinetic Parameters in the Reaction of Different Carbon materials with Oxygen. *Energy Fuels* **1993**, *7*, 1141–1145.
- (13) Várhegyi, G.; Antal, M. J., Jr.; Székely, T.; Till, F.; Jakab, E.: Simultaneous Thermogravimetric - Mass Spectrometric Studies on the Thermal Decomposition of Biopolymers. *Energy Fuels* **1988**, *2*, 267–277
- (14) Várhegyi, G.; Antal, M. J., Jr.; Székely, T.; Szabó: Kinetics of the Thermal Decomposition of Cellulose, Hemicellulose and Sugar Cane Bagasse. *Energy Fuels* **1989**, *3*, 329–335.
- (15) Várhegyi, G.; Jakab, E.; Antal, M. J., Jr.: Is the Broido - Shafizadeh Model for Cellulose Pyrolysis True? *Energy Fuels* **1994**, *8*, 1345–1352
- (16) Várhegyi, G.; Szabó, P.; Mok, W. S. L.; Antal, M. J., Jr.: Kinetics of the thermal decomposition of cellulose in sealed vessels at elevated pressures. Effects of the presence of water on the reaction mechanism. *J. Anal. Appl. Pyrol.* **1993**, *26*, 159–174.
- (17) Chornet, E.; Baldasano, J. M.; Tarki, H. T.: Kinetic expressions for coal char–gas reactions, *Fuel* **1979**, *58*, 395–396
- (18) Hill, M.; Fott, P.: Kinetics of gasification of Czech brown coals. *Fuel* **1993**, *72*, 525–529.
- (19) Duval, C. *Inorganic Thermogravimetric Analysis*. Elsevier, The Netherlands, 1963.
- (20) Su, J.–L.; Perlmutter, D. D.: Effect of Pore Structure on Char Oxidation. *AIChE J.* **1985**, *31*, 973–981.
- (21) Floess, J. K.; Longwell, J. P.; Sarofim, A. F.: Intrinsic Reaction-Kinetics of Microporous Carbons. 1. Noncatalyzed Chars. *Energy Fuels* **1988**, *2*, 18–26.
- (22) Gopalakrishnan, R.; Fullwood, M. J.; Bartholomew, C. H.: Catalysis of Char Oxidation by Calcium Minerals: Effect of Calcium Compound Chemistry on the Intrinsic Reactivity of Doped Spherochar and Zap Chars. *Energy Fuels* **1994**, *8*, 984–989.
- (23) Álvarez, T.; Fuertes, A. B.; Pis, J. J.; Ehrburger, P.: Influence of Coal Oxidation upon Char Gasification Reactivity. *Fuel* **1995**, *74*, 729–735.
- (24) Chi, W.–K.; Perlmutter, D. D.: Effect of Pore Structure on Char–Steam Reaction. *AIChE J.* **1989**, *35*, 1791–1802.
- (25) Jessen, T. and Sorensen, L. H.: The Unipore Model. Pore Evolution in Kinetically Controlled Gas–Solid Reactions. in: “Nordic Seminar on Combustion and Gasification Reactivities of Solid Fuels”, (Ed. by Johan Hustad) VTT, Jyväskylä, 1993, Chapter 8, pp. 1–5.